A NONORTHOGONAL FINITE-VOLUME METHOD FOR THE SOLUTION OF ALL SPEED FLOWS USING CO-LOCATED VARIABLES

C. H. Marchi and C. R. Maliska
Computational Fluid Dynamics Laboratory—SINMEC,
Department of Mechanical Engineering, Federal University of Santa Catarina,
P.O. Box 476, 88040-900, Florianópolis, SC, Brazil

The use of the segregated finite-volume method requires special procedures for handling the pressure–velocity coupling. It is a normal practice to employ staggered grids to promote the adequate coupling between pressure and velocity. However, this alternative becomes unfeasible for three-dimensional problems, especially if boundary-fitted grids are employed. In this work a numerical model employing co-located variables is developed. The model uses nonorthogonal boundary-fitted meshes and is therefore suitable for the solution of all speed flows, considering the extra coupling between pressure and density. Results are obtained for selected test cases, including incompressible as well as supersonic flows, which are compared with experimental ones.

INTRODUCTION

The prediction of the fluid flow motion and the heat transfer rates involved in many important engineering devices requires the solution of a coupled set of nonlinear partial differential equations representing conservation of mass, momentum, and energy. General methods for the solution of these equations are still a challenging task for fluid dynamics theoreticians. In recent years there has been a formidable amount of work in developing numerical models for the solution of fluid flow problems in complex geometries. Boundary-fitted nonorthogonal methods, after the pioneering works of Chu [1], Winslow [2], and Thompson et al. [3, 4], have become a widely used technique for handling arbitrary geometries. In the aerospace engineering branch, dealing mostly with the solution of transonic and supersonic flows, boundary-fitted methods are used extensively in conjunction with finite-difference-based methods. In thermal engineering, dealing mostly with incompressible flows, boundary-fitted nonorthogonal methods are also widely employed, using the finite-volume concept, and generally adopting the staggered grid concept of Harlow and Welch [5] for promoting an adequate coupling between velocity and pressure.

Received 4 February 1994; accepted 25 April 1994.
Address correspondence to C. R. Maliska, Computational Fluid Dynamics Laboratory—SINMEC, Department of Mechanical Engineering, Federal University of Santa Catarina, P.O. Box 476, 88040-900, Florianópolis, SC, Brazil.

Numerical Heat Transfer, Part B, 26:293–311, 1994

1040–7790/94 $10.00 + .00

NOMENCLATURE

a	coefficients in the momentum and energy equations	U, V	contravariant components of the velocity vector
A	coefficients for the pressure correction equation	x_1, x_2	coordinates in the Cartesian/cylindrical coordinate system
b	source term for the momentum and energy equations	$\overline{\alpha}, \overline{\beta}$	coefficients in the WUDS scheme
B	source term for the pressure correction equation	α, β, γ	components of the metric tensor
c_p	specific heat at constant pressure	$\overline{\gamma}$	coefficient in the UDS scheme
d	coefficient in the velocity correction equation	Γ	diffusion coefficient
J	Jacobian of the transformation	Δt	time step
k	thermal conductivity	μ	viscosity
M	mass inside the control volume	ξ, η	coordinates in the general curvilinear coordinate system
$\dot{M}$	mass flux	ρ	density
p	pressure	ϕ	scalar field
p'	pressure correction	**Subscripts**	
P^ϕ	pressure source term in the equation for ϕ	e, w, n, s	denotes control volume interfaces
$\hat{P}^\phi$	transformed pressure source term in the equation for ϕ	P, E, W, N, S, NE, SE, NW, SW	denotes the center of the control volumes
R	gas constant		
S^ϕ	source term in the equation for ϕ		
$\hat{S}^\phi$	transformed source term in the equation for ϕ	ξ, η	partial derivatives of first order
t	time	**Superscripts**	
T	temperature		
u, v	Cartesian components of the velocity vector	$^\circ$	denotes quantity evaluated at the previous time level

The staggered grid, in spite of producing an adequate coupling, introduces an extremely cumbersome computer code implementation, especially for three-dimensional problems. The need for staggered control volumes requires the calculation of different flow areas for computing the convective and diffusive fluxes, implying additional storage for the geometric information. In addition, boundary conditions applications are also more difficult and more elaborate if the control volumes are not coincident. These drawbacks have motivated recent research work in the development of co-located methods by Rhie [6], Hsu [7], Reggio and Camarero [8], Peric et al. [9], and Majundar [10], among others. The co-located techniques are starting to become a currently used tool, as in Melaaen [11] and Chen and Pletcher [12]. These methods, however, have been applied mainly to incompressible flows, where the important coupling is between pressure and velocity.

This article presents a numerical model, designed in the framework of a boundary-fitted coordinate system, using co-located variables, for the solution of incompressible as well as compressible flows. The co-location technique follows the idea presented in Marchi et al. [13]. In the case of compressible flows, the coupling is now between velocity/density and pressure, and the approach for handling all

speed flows follows the idea presented in Patankar [14] and in Harlow and Amsden [15], and further explored in Van Doormaal [16] for one- and two-dimensional flows in Cartesian coordinates, in Silva and Maliska [17], Maliska and Silva [18], and Karki and Patankar [19] for two-dimensional nonorthogonal boundary-fitted grids, and in Marchi et al. [20] for three-dimensional flows.

The method is tested by solving fluid flow problems in the incompressible limit as well as truly compressible flows with strong shocks. These problems are chosen with the aim of comparing the performance of the co-located and the staggered arrangements.

GOVERNING EQUATIONS

The governing equations for laminar compressible flow with constant physical properties can be written for a general scalar ϕ in the Cartesian and cylindrical coordinate systems as [17]

$$\frac{\partial}{\partial t}(\rho\phi) + \frac{\partial}{\partial x_1}(\rho u\phi) + \frac{1}{x_2^j}\frac{\partial}{\partial x_2}(\rho x_2^j v\phi)$$

$$= \Gamma^\phi \frac{\partial}{\partial x_1}\left(\frac{\partial\phi}{\partial x_1}\right) + \frac{\Gamma^\phi}{x_2^j}\frac{\partial}{\partial x_2}\left(x_2^j\frac{\partial\phi}{\partial x_2}\right) - P^\phi + S^\phi \qquad (1)$$

where ϕ, Γ^ϕ, P^ϕ, and S^ϕ are shown in Table 1. Planar and axisymmetric flows can be handled by putting $j = 0$ and $j = 1$, respectively, in Eq. (1). The ϕ variable represents the mass conservation equation, the two Cartesian/cylindrical velocity components, and the energy equation, being equal to 1, u, v, and T, respectively.

Equation (1) can be transformed to the general curvilinear coordinate system by employing the chain rule. After some algebraic manipulations in order to put

Table 1. Expressions for P^ϕ and S^ϕ

ϕ	Γ^ϕ	P^ϕ	S^ϕ
1	0	0	0
u	μ	$\dfrac{\partial p}{\partial x_1}$	$\dfrac{\mu}{3}\dfrac{\partial}{\partial x_1}(\vec{\nabla}\cdot\vec{\mathbf{V}})$
v	μ	$\dfrac{\partial p}{\partial x_2}$	$\dfrac{\mu}{3}\dfrac{\partial}{\partial x_2}(\vec{\nabla}\cdot\vec{\mathbf{V}}) - \dfrac{j\mu v}{x_2^2}$
T	k/c_p	$-\dfrac{1}{c_p}\left[\dfrac{\partial p}{\partial t}\right.$	$\dfrac{\mu}{c_p}\left\{2\left[\left(\dfrac{\partial u}{\partial x_1}\right)^2 + \left(\dfrac{\partial v}{\partial x_2}\right)^2 + j\left(\dfrac{v}{x_2}\right)^2\right]\right.$
		$\left. + \nabla\cdot(p\mathbf{V}) - p(\nabla\cdot\mathbf{V})\right]$	$\left. + \left(\dfrac{\partial v}{\partial x_1} + \dfrac{\partial u}{\partial x_2}\right)^2 - \dfrac{2}{3}(\nabla\cdot\mathbf{V})^2\right\}$

the equation in the conservative form, Eq. (1) reads

$$\frac{1}{J}\frac{\partial}{\partial t}(\rho\phi) + \frac{1}{x_2^j}\frac{\partial}{\partial \xi}(\rho x_2^j U\phi) + \frac{1}{x_2^j}\frac{\partial}{\partial \eta}(\rho x_2^j V\phi)$$

$$= -\hat{P}^\phi + \hat{S}^\phi + \frac{\Gamma^\phi}{x_2^j}\frac{\partial}{\partial \xi}\left(x_2^j \alpha J \frac{\partial \phi}{\partial \xi} - x_2^j \beta J \frac{\partial \phi}{\partial \eta}\right)$$

$$+ \frac{\Gamma^\phi}{x_2^j}\frac{\partial}{\partial \eta}\left(x_2^j \gamma J \frac{\partial \phi}{\partial \eta} - x_2^j \beta J \frac{\partial \phi}{\partial \xi}\right) \tag{2}$$

where

$$U = (x_2)_\eta u - (x_1)_\eta v \tag{3}$$

$$V = (x_1)_\xi v - (x_2)_\xi u \tag{4}$$

$$\alpha = (x_1)_\eta^2 + (x_2)_\eta^2 \tag{5}$$

$$\gamma = (x_1)_\xi^2 + (x_2)_\xi^2 \tag{6}$$

$$\beta = (x_1)_\xi (x_1)_\eta + (x_2)_\xi (x_2)_\eta \tag{7}$$

$$J = \left[(x_1)_\xi (x_2)_\eta - (x_1)_\eta (x_2)_\xi\right]^{-1} \tag{8}$$

The expressions for $\hat{P}^\phi$ and $\hat{S}^\phi$ are presented in Table 2. As can be seen, the Cartesian velocity components are kept as dependent variables [21].

Table 2. Expressions for $\hat{P}^\phi$ and $\hat{S}^\phi$

ϕ	$\hat{P}^\phi$	$\hat{S}^\phi$
1	0	0
u	$\frac{\partial p}{\partial \xi}(x_2)_\eta - \frac{\partial p}{\partial \eta}(x_2)_\xi$	$\frac{\mu}{3}\left[(x_2)_\eta \frac{\partial}{\partial \xi}(\nabla\cdot\mathbf{V}) - (x_2)_\xi \frac{\partial}{\partial \eta}(\nabla\cdot\mathbf{V})\right]$
v	$\frac{\partial p}{\partial \eta}(x_1)_\xi - \frac{\partial p}{\partial \xi}(x_1)_\eta$	$\frac{\mu}{3}\left[(x_1)_\xi \frac{\partial}{\partial \eta}(\nabla\cdot\mathbf{V}) - (x_1)_\eta \frac{\partial}{\partial \xi}(\nabla\cdot\mathbf{V})\right] - \frac{j\mu v}{Jx_2^2}$
		$= \frac{\mu}{c_P}\left(2J\left\{\left[(x_2)_\eta \frac{\partial u}{\partial \xi} - (x_2)_\xi \frac{\partial u}{\partial \eta}\right]^2\right.\right.$
T	$-\frac{1}{c_P J}\left[\frac{\partial p}{\partial t} + \nabla\cdot(p\mathbf{V})\right.$	$\left.+\left[(x_1)_\xi \frac{\partial v}{\partial \eta} - (x_{1_\eta})\frac{\partial v}{\partial \xi}\right]^2\right\} + \frac{2j}{J}(\frac{v}{x_2})^2$
	$\left. - p(\nabla\cdot\mathbf{V})\right]$	$+J\left\{\frac{\partial}{\partial \xi}[v(x_2)_\eta - u(x_1)_\eta]\right.$
		$\left.\left.+\frac{\partial}{\partial \eta}[u(x_1)_\xi - v(x_2)_\xi]\right\}^2 - \frac{2}{3J}(\nabla\cdot\mathbf{V})^2\right)$

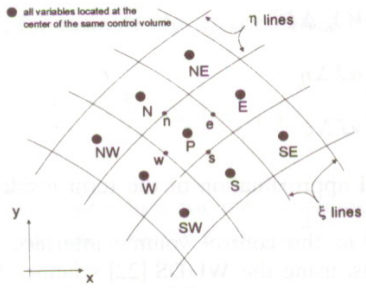

(a)

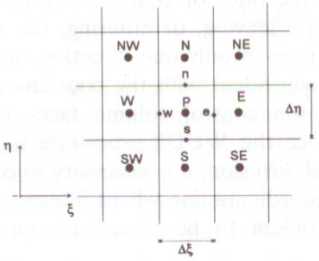

(b)

Figure 1. (*a*) Physical domain. (*b*) Computational domain.

DISCRETIZED EQUATIONS

Momentum and Energy Equations

To obtain the discretized equations using the finite-volume concept, Eq. (1) is integrated over the irregular elemental control volume, Figure 1*a*, or Eq. (2) is integrated over the regular elemental volume in the (ξ, η) domain, Figure 1*b*. Since one is dealing with structured grids, the latter strategy is simpler and, therefore, preferred. Integration in space and in time results in

$$\frac{M_P \phi_P - M_P^\circ \phi_P^\circ}{\Delta t} + \dot{M}_e \phi_e - \dot{M}_w \phi_w + \dot{M}_n \phi_n - \dot{M}_s \phi_s$$

$$= -L[\hat{P}^\phi]_P \, \Delta V + L[\hat{S}^\phi]_P \, \Delta V + \left[D_1 \frac{\partial \phi}{\partial \xi} + D_2 \frac{\partial \phi}{\partial \eta} \right]_e$$

$$- \left[D_1 \frac{\partial \phi}{\partial \xi} + D_2 \frac{\partial \phi}{\partial \eta} \right]_w + \left[D_3 \frac{\partial \phi}{\partial \eta} + D_4 \frac{\partial \phi}{\partial \xi} \right]_n - \left[D_3 \frac{\partial \phi}{\partial \eta} + D_4 \frac{\partial \phi}{\partial \xi} \right]_s \quad (9)$$

where $\dot{M}_e$ and $\dot{M}_n$, D_1 and D_3, for example, are given by

$$\dot{M}_e = (x_2^j \rho U)_e \, \Delta \eta \quad (10)$$

$$\dot{M}_n = (x_2^j \rho V)_n \Delta\xi \tag{11}$$

$$D_1 = \Gamma^\phi x_2^j \alpha J \Delta\eta \tag{12}$$

$$D_3 = \Gamma^\phi x_2^j \gamma J \Delta\xi \tag{13}$$

and the notation L[ ] means the numerical approximation of the term inside the brackets.

The values of ϕ and its derivatives at the control volume interfaces are evaluated, as a function of the nodal points, using the WUDS [22] scheme. As is well known, the WUDS scheme weights the diffusion and convection fluxes along one coordinate direction in order to establish the value of ϕ at the interfaces. For orthogonal grids the total flux of the property leaving, or entering, the surface control volume can be represented by derivatives in only one direction, since the normals to the control volume surfaces are coincident with the coordinate lines. For nonorthogonal grids the flux crossing the control volume faces involves derivatives in both coordinate directions. Since the WUDS procedure is a one-dimensional weighting between convection and diffusion, it is necessary to consider only the part of the diffusive flux along the coordinate line where interpolation is being done. Then, the one-dimensional problem to be solved to obtain the interpolation function is

$$\frac{\partial}{\partial\xi}(\rho U\phi) = \Gamma^\phi \frac{\partial}{\partial\xi}\left(\alpha J \frac{\partial\phi}{\partial\xi}\right) \tag{14}$$

Using the usual procedure to establish boundary conditions for the above equation, the values of ϕ and its derivatives, for example, for the east face are given by

$$\phi_e = \left(\frac{1}{2} + \bar{\alpha}_e\right)\phi_P + \left(\frac{1}{2} - \bar{\alpha}_e\right)\phi_E \tag{15}$$

$$\left(\frac{\partial\phi}{\partial\xi}\right)_e = \bar{\beta}_e \frac{(\phi_E - \phi_P)}{\Delta\xi} \tag{16}$$

where expressions for $\bar{\alpha}$ and $\bar{\beta}$ can be found in [23]. Introducing Eqs. (15)–(16), and the corresponding ones for the remaining faces of the control volume, in Eq. (9), one gets

$$a_P\phi_P = \sum(a_{nb}\phi_{NB})_P + L[\hat{S}^\phi]_P \Delta V - L[\hat{P}^\phi]_P \Delta V + \frac{M_P^\circ \phi_P^\circ}{\Delta t} \tag{17}$$

where

$$\sum(a_{nb}\phi_{NB})_P = a_e\phi_E + a_w\phi_W + a_n\phi_N + a_s\phi_S + a_{ne}\phi_{NE} + a_{se}\phi_{SE} + a_{nw}\phi_{NW} + a_{sw}\phi_{SW} \tag{18}$$

where, for example, the a_e coefficient is given by

$$a_e = -\left(\frac{1}{2} - \bar{\alpha}_e\right)\dot{M}_e + \Gamma^{\phi}\left(\bar{\beta}x_2^j \alpha J\right)_e - \frac{\Gamma^{\phi}}{4}\left[(x_2^j \beta J)_n - (x_2^j \beta J)_s\right] \quad (19)$$

The expressions for the remaining coefficients of Eq. (17) are given in the Appendix. The pressure term, $L[\hat{P}^{\phi}]_P$, for the u-momentum equation is given by

$$L[\hat{P}^u]_P = \frac{(p_E - p_W)}{2\,\Delta\xi}(x_{2\eta})_P - \frac{(p_N - p_S)}{2\,\Delta\eta}(x_{2\xi})_P \quad (20)$$

As can be seen in the above equation, a central differencing scheme is used for the pressure gradient in the momentum equations due to the co-located arrangement of the variables. At this point it is important to mention that the way the pressure gradient is evaluated in the momentum equation is not the key question for promoting strong coupling between pressure and velocity. Rather, of utmost importance is the way it is evaluated in the velocity-correction equations. In these equations it is imperative that a consistent pressure gradient be employed.

Mass Conservation Equation

The discretized form of the mass conservation equation can be obtained from Eq. (9), putting $\phi = 1$ and the pressure and source terms equal to zero. The resulting equation reads

$$\frac{(M_P - M_P^{\circ})}{\Delta t} + \dot{M}_e - \dot{M}_w + \dot{M}_n - \dot{M}_s = 0 \quad (21)$$

In the incompressible formulation, or when ρ is a function of temperature only, the mass conservation equation can no longer be used as an equation for density. In these cases the mass conservation equation is transformed into an equation for pressure, with the density constant or calculated through a state equation as a function of temperature. This approach requires the well-known treatment of the pressure/velocity coupling when segregated solutions are employed [24, 25]. For high-Mach-number flows the above-mentioned procedure can no longer be used, since density now needs to be kept active in the mass conservation equation. The approach of using the mass conservation equation as an equation for density, encountered largely in the solution of supersonic flows, also does not suffice, since it cannot be applied for low-Mach-number flows.

It seems, therefore, that both density and velocity must be kept active [14–17] in the mass conservation equation in order to have a methodology able to solve all speed flows. In this work the method described in [17, 18] is employed. Density and velocity are kept active in the mass conservation equation through a special

linearization in the mass fluxes [16]. Taking $\dot{M}_e$ as example, the linearization has the form

$$\dot{M}_e = (x_2^j)_e(\rho U^* + \rho^* U - \rho^* U^*)_e \Delta\eta \tag{22}$$

where ρ^* and U^* are best estimated values, and ρ and U are unknowns.

An analysis of Eq. (22) reveals that when velocity plays no important role in the mass conservation equation, such that it could be put into the coefficients, the second and third terms on the right-hand side cancel out, leaving the first term, representing the linearization used when high-Mach-number flows are solved. When density plays no important role, the first and third terms cancel out, recovering the linearization for low-Mach-number flows.

Introducing Eq. (22) and its counterparts for the other faces of the control volume into Eq. (21), one gets

$$\begin{aligned}&\frac{(M_P - M_P^\circ)}{\Delta t} + \left[(x_2^j \rho U^*)_e - (x_2^j \rho U^*)_w + (x_2^j \rho^* U)_e - (x_2^j \rho^* U)_w\right]\Delta\eta \\ &\quad + \left[(x_2^j \rho V^*)_n - (x_2^j \rho V^*)_s + (x_2^j \rho^* V)_n - (x_2^j \rho^* V)_s\right]\Delta\xi \\ &\quad - \left[(x_2^j \rho^* U^*)_e - (x_2^j \rho^* U^*)_w\right]\Delta\eta - \left[(x_2^j \rho^* V^*)_n - (x_2^j \rho^* V^*)_s\right]\Delta\xi = 0\end{aligned} \tag{23}$$

Equation (23) now needs to be converted into an equation for pressure. Therefore, ρ, U, and V need to be replaced by functions of pressure. The substitution of U and V by functions of pressure gives rise to the velocity-correction equations, characterizing the velocity–pressure coupling. The replacement of density as function of pressure gives rise to the density-correction equation, introducing a new coupling. The full coupling can be now called velocity/density–pressure coupling, since now pressure dictates the changing of velocity and density in the mass conservation equation.

Following the SIMPLEC [26] procedure, the corrections for the u and v velocity components at the control volume interface are given by

$$u_e = u_e^* - d_e L[\hat{P}'^u]_e \Delta\xi \tag{24}$$

$$v_e = v_e^* - d_e L[\hat{P}'^v]_e \Delta\xi \tag{25}$$

where $p' = p - p^*$.

Using the relation between the contravariant and Cartesian velocity components, one gets

$$U_e = U_e^* - d_e\left(\alpha \frac{\Delta p'}{\Delta\xi} - \beta \frac{\Delta p'}{\Delta\eta}\right)_e \Delta\xi \tag{26}$$

$$U_w = U_w^* - d_w\left(\alpha \frac{\Delta p'}{\Delta\xi} - \beta \frac{\Delta p'}{\Delta\eta}\right)_w \Delta\xi \tag{27}$$

$$V_n = V_n^* - d_n\left(\gamma\frac{\Delta p'}{\Delta\eta} - \beta\frac{\Delta p'}{\Delta\xi}\right)_n \Delta\eta \tag{28}$$

$$V_s = V_s^* - d_s\left(\gamma\frac{\Delta p'}{\Delta\eta} - \beta\frac{\Delta p'}{\Delta\xi}\right)_s \Delta\eta \tag{29}$$

Since we are using co-located variables, neither U nor V is stored at the control volume interfaces. The way these velocities are calculated is discussed later.

To obtain an expression for density, the linearized state equation must be used. Following [16, 17], the density correction equation is

$$\rho = \rho^* + C^\rho p' \tag{30}$$

Equation (23) requires ρ at the interfaces of the control volume for mass conservation. It should then be interpolated using the nodal values. The interpolation is done using an equation similar to Eq. (15) with the weighting parameter ($\bar{\gamma}$) equal to $+0.5$ (if U or $V \geq 0$) or -0.5 (if U or $V < 0$) [16]. This assures positive coefficients for the mass conservation equation. In this manner an upstream scheme is used for density, that is,

$$\rho_e = \left(\frac{1}{2} + \bar{\gamma}_e\right)\rho_P + \left(\frac{1}{2} - \bar{\gamma}_e\right)\rho_E \tag{31}$$

$$\rho_n = \left(\frac{1}{2} + \bar{\gamma}_n\right)\rho_P + \left(\frac{1}{2} - \bar{\gamma}_n\right)\rho_N \tag{32}$$

with similar equations for the remaining faces of the control volume. In Eqs. (31)–(32), ρ_P, ρ_E, and ρ_N are obtained from Eq. (30). Introducing Eqs. (26)–(29) and Eqs. (31)–(32) and their analogs into Eq. (23), one obtains the equation for pressure correction in the following form:

$$A_P p'_P = \sum(A_{nb} p'_{NB}) + B_P \tag{33}$$

where

$$\sum(A_{nb} p'_{NB}) = A_e p'_E + A_w p'_W + A_n p'_N + A_s p'_S \tag{34}$$

where the expression for the coefficients and for B_P can be seen in the Appendix. Solving Eq. (33) for pressure correction, the density and velocity fields can be corrected such that mass is conserved. It is to be noted that the pressure-correction equation, Eq. (33), is of the five-point form, since only the principal pressure gradient terms were retained in the velocity correction equations, Eqs. (26)–(29). This makes the computational code considerably simpler, especially in three dimensions. Furthermore, neglecting the transversal pressure gradient terms in the velocity-correction equations can affect only the convergence rate. Studies undertaken in solving three-dimensional all-speed flows [20] demonstrated that the convergence rate was not altered when the terms were neglected.

Determination of U^* and V^* at the Interfaces

Since we are using co-located variables, and U^* and V^* are required at the interfaces of the control volumes, interpolation needs to be used to find these velocities. The easiest way of finding U_e^*, for example, would be through a linear interpolation between u_P^* and u_E^*, and v_P^* and v_E^* (see Figure 2). This is not recommended because it provides a poor coupling between velocity and pressure. Instead, it is wise to create a pseudo-momentum equation for the Cartesian velocities at the interfaces, through an average of the momentum equations at the nearest nodal points. In this work is proposed a scheme akin to the one described in [9] but with better convergence characteristics. Rewriting the momentum equation, Eq. (17), for the u velocity at the P and E control volumes, one gets

$$(a_P)_P u_P^* = \sum (a_{nb} u_{NB}^*)_P + L[\hat{S}^{*u}]_P \, \Delta V + \frac{M_P^\circ u_P^\circ}{\Delta t} - L[\hat{P}^{*u}]_P \, \Delta V \tag{35}$$

$$(a_P)_E u_E^* = \sum (a_{nb} u_{NB}^*)_E + L[\hat{S}^{*u}]_E \, \Delta V + \frac{M_E^\circ u_E^\circ}{\Delta t} - L[\hat{P}^{*u}]_E \, \Delta V \tag{36}$$

where $(a_P)_P$ and $(a_P)_E$ represent the central coefficients for the velocities at P and E, respectively. Interpolating linearly Eqs. (35)–(36), except for the two last terms of each equation, one obtains

$$u_e^* = \Big[\sum (a_{nb} u_{NB}^*)_P + \sum (a_{nb} u_{NB}^*)_E + L[\hat{S}^{*u}]_P \, \Delta V + L[\hat{S}^{*u}]_E \, \Delta V + (M_P^\circ + M_E^\circ) u_e^\circ / \Delta t - 2L[\hat{P}^{*u}]_e \, \Delta V \Big] / [(a_P)_P + (a_P)_E] \tag{37}$$

Observe that the pressure gradient in Eq. (37) is evaluated at the interface, and so a consistent pressure gradient can be obtained. The evaluation of u_e through Eq. (37) guarantees that the steady-state solutions are independent of the Δt employed.

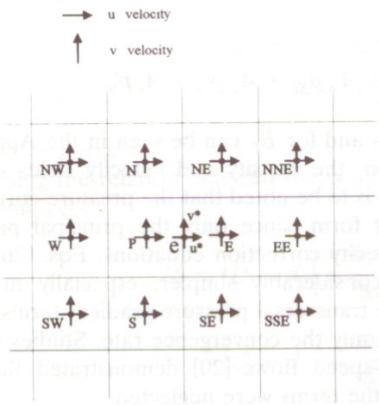

Figure 2. u and v velocities involved in the calculation of u_e^* and v_e^*.

Using the same procedure, v_e^* can also be found. Knowing u_e^* and v_e^*, the U_e^* contravariant component can also be calculated. In the same manner, U_w^*, V_n^*, and V_s^* can be found and substituted into the source term for p'.

SOLUTION PROCEDURE

1. If a true transient is to be followed, all variables are known at a time level n.
2. Calculate the coefficients and source terms for u and v. Solve the corresponding linear systems, Eq. (17), obtaining u^* and v^*.
3. Interpolate u^* and v^* using equations like Eq. (37) to obtain U^* and V^* at the interfaces.
4. Calculate the coefficients and source term for p'. Solve Eq. (33) for p'.
5. Correct the contravariant velocity components with the Eqs. (26)–(29) and the density with Eq. (30).
6. Correct u^* and v^* at nodal points with expressions akin to Eqs. (24)–(25). At this point several alternatives are possible. If one wants to solve the u, v, ρ, p coupling for a given set of coefficients, cycling back to step 2, computing only the new source term involving pressure, is necessary. If the nonlinearities are also taken into account, the coefficients should also be calculated in step 2.
7. Solve for temperature. Using the state equation, calculate new densities.
8. Return to step 2 and iterate until convergence is achieved. At this point the solution is known for the time level $n + 1$.
9. Repeat the procedure until steady state is reached or until the solution is as desired.

TEST PROBLEMS

The main objective of the following tests is to compare the performance of the numerical schemes using co-located and staggered variables. The staggered arrangement employed for the solution of the test problems is described in [17, 18] and was fully tested previously. Since the model can solve all speed flows, we have included incompressible as well as compressible flows with strong shocks in the testing procedure.

Incompressible Flow in the Entrance Region of Parallel Plates

The first test problem is the laminar incompressible flow in the entrance region of two parallel plates. The Mach number was taken equal to 5×10^{-5} in order to have a truly incompressible flow. The Reynolds number based on the distance between the plates was taken equal to 5. Figure 3 shows the axial velocity profile for different locations using staggered and co-located variables. The results are coincident. Remember that the entrance flow is a two-dimensional problem with a nonzero v velocity, which requires the mass conservation equation to be locally satisfied, which is in turn intimately connected with the way variables are

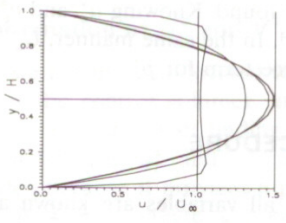

Figure 3. Velocity profiles for different axial stations for $M = 5 \times 10^{-5}$ and $\mathrm{Re}_h = 5$.

located on the grid. Although apparently simple, this problem serves to demonstrate the ability of the model to solve very-low-Mach-number flows as well as the time-step independence of the co-located algorithm. The CPU effort to obtain the solution using both arrangements is the same. A 22×18 grid was used to obtain the solution.

Compressible Flow over an Obstacle

The second test problem is the supersonic flow over an obstacle [16], as shown in Figure 4. The constant-pressure lines for this problem are shown in Figure 5*a* for both variable arrangements for a 22×18 mesh. It can be seen that behind the obstacle the agreement is not good. The discrepancies, however, are not due to a failure of any arrangement, but due to the coarseness of the mesh. Figure 5*b* demonstrates this, where both results agree well when a 44×36 grid is used. Figure 6 shows the convergence behavior as a function of the size of the time step, for both arrangements.

An important finding is the fact that both grid arrangements have the same minimum CPU effort for almost the same time step, besides the fact that the staggered arrangement offers a wider range of time steps where convergence can still be achieved.

Compressible Flow over a Launch Vehicle

As a final test, the supersonic flow over the forebody of the Brazilian launch vehicle (VLS) shown in Figure 7*a* is solved using the Euler equations for zero angle

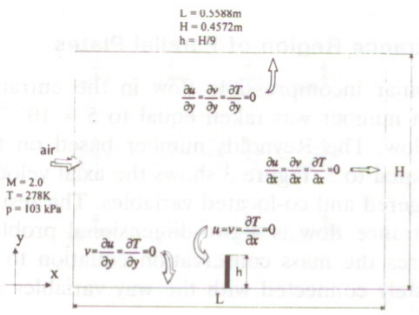

Figure 4. Geometry and boundary conditions. Flow over obstacle.

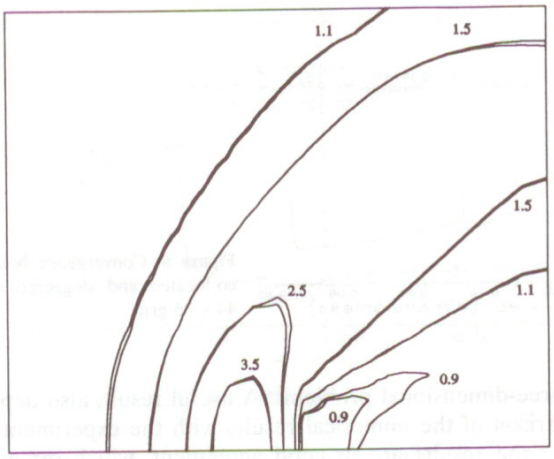

(*a*)

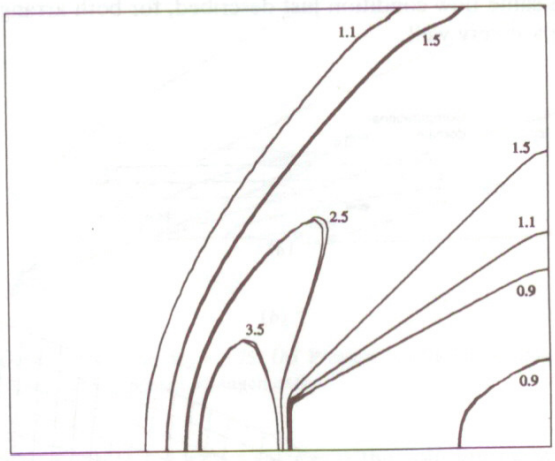

(*b*)

Figure 5. (*a*) Constant-pressure lines. Co-located and staggered arrangements. 22 × 18 grid. (*b*) Constant-pressure lines. Co-located and staggered arrangements. 44 × 36 grid.

of attack and Mach number of 3.75. The 60 × 24 grid employed is shown in Figure 7*b*, where all the appropriate boundary conditions used are listed. The grid was generated algebraically considering a hyperbole as outer boundary.

Figure 8*a* shows the numerical results for the pressure coefficient for co-located and staggered arrangements. The results are coincident and are represented by a unique solid line. Since the staggered arrangement is a fully tested variable layout even in three-dimensional situations, the good agreement obtained with the co-located arrangement encourages the implementation of the proposed

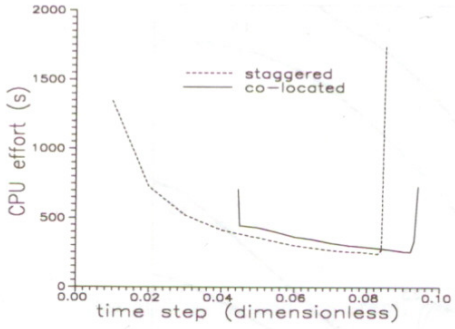

Figure 6. Convergence behavior for the co-located and staggered arrangements. 44× 36 grid.

procedure for three-dimensional problems. A useful result, also depicted in Figure 8*a*, is the comparison of the numerical results with the experimental ones [27]. It can be seen that the results are in good agreement, which serves as an overall assessment of the full methodology. Figure 8*b* shows the pressure coefficient contours for the same flow condition just described, for both arrangements. Again, the results compare very well.

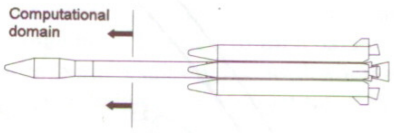

(*a*)

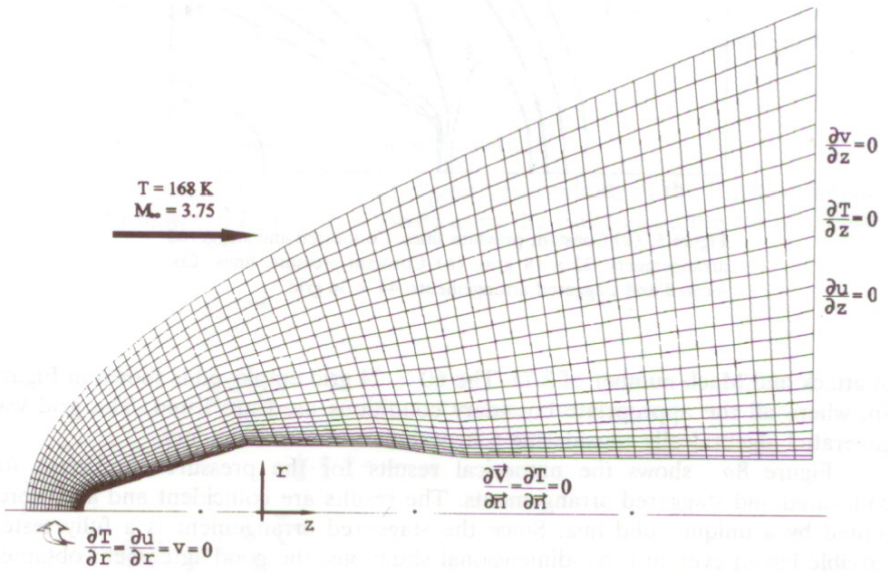

(*b*)

Figure 7. (*a*) Full configuration of the VLS vehicle. (*b*) 60 × 24 grid over the VLS fairing.

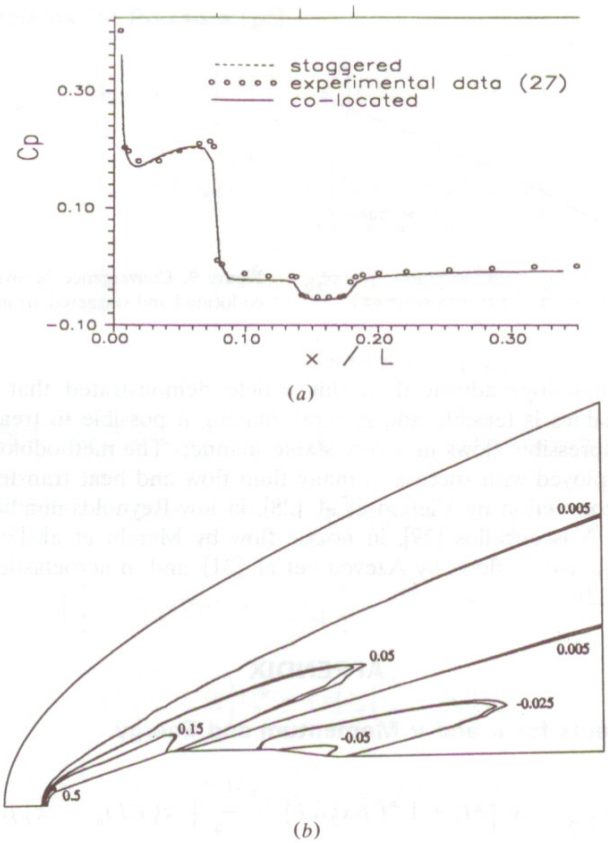

Figure 8. (*a*) C_p for $M_\infty = 3.75$. (*b*) Pressure coefficient contours. Co-located and staggered arrangements.

Finally, the computational effort to obtain the solution to the same level of convergence is depicted in Figure 9. Two findings are noteworthy. The computational effort necessary for the staggered arrangement is about 60% greater than the one required by the co-located layout in the minimum CPU effort, and the range of time steps to achieve convergence is wider for the latter arrangement.

CONCLUDING REMARKS

The use of the staggered grid arrangement has remained as the alternative for treating the pressure–velocity coupling in the solution of incompressible fluid flow problems for more than two decades. For three-dimensional codes, however, its implementation is complex and cumbersome, especially if boundary-fitted meshes are employed, due to extra computational storage required for the geometric information about the different control volumes. Therefore, the staggered approach needs to be replaced by co-located schemes for structured and unstructured grids.

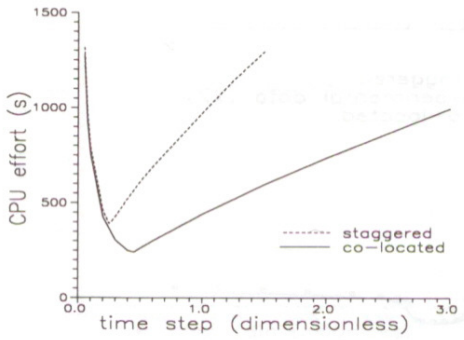

Figure 9. Convergence behavior for the co-located and staggered arrangements.

The methodology advanced in this article demonstrated that the use of co-located variables is feasible and general, making it possible to treat compressible and incompressible flows in a very stable manner. The methodology has been extensively employed with success in many fluid flow and heat transfer problems, as in natural convection by Vielmo et al. [28], in low-Reynolds-number turbulent flows (κ-ε) by Vasconcellos [29], in nozzle flow by Marchi et al. [30], in three-dimensional supersonic flows by Azevedo et al. [31], and in aeroelastic analysis by Bortoli et al. [32].

APPENDIX

Coefficients for *u* and *v* Momentum and Energy

$$a_e = -\left(\frac{1}{2} - \bar{\alpha}_e\right)\dot{M}_e + \Gamma^\phi\left(\bar{\beta}x_2^j\alpha J\right)_e - \frac{\Gamma^\phi}{4}\left[(x_2^j\beta J)_n - (x_2^j\beta J)_s\right]$$

$$a_n = -\left(\frac{1}{2} - \bar{\alpha}_n\right)\dot{M}_n + \Gamma^\phi\left(\bar{\beta}x_2^j\gamma J\right)_n - \frac{\Gamma^\phi}{4}\left[(x_2^j\beta J)_e - (x_2^j\beta J)_w\right]$$

$$a_w = \left(\frac{1}{2} + \bar{\alpha}_w\right)\dot{M}_w + \Gamma^\phi\left(\bar{\beta}x_2^j\alpha J\right)_w - \frac{\Gamma^\phi}{4}\left[(x_2^j\beta J)_s - (x_2^j\beta J)_n\right]$$

$$a_s = \left(\frac{1}{2} + \bar{\alpha}_s\right)\dot{M}_s + \Gamma^\phi\left(\bar{\beta}x_2^j\gamma J\right)_s - \frac{\Gamma^\phi}{4}\left[(x_2^j\beta J)_w - (x_2^j\beta J)_e\right]$$

$$a_{ne} = -\frac{\Gamma^\phi}{4}\left[(x_2^j\beta J)_e + (x_2^j\beta J)_n\right] \qquad a_{se} = \frac{\Gamma^\phi}{4}\left[(x_2^j\beta J)_e + (x_2^j\beta J)_s\right]$$

$$a_{sw} = -\frac{\Gamma^\phi}{4}\left[(x_2^j\beta J)_w + (x_2^j\beta J)_s\right] \qquad a_{nw} = \frac{\Gamma^\phi}{4}\left[(x_2^j\beta J)_w + (x_2^j\beta J)_n\right]$$

$$a_P = \frac{M_P^\circ}{\Delta t} + a_e + a_w + a_n + a_s$$

Coefficients for Pressure (p')

$$A_e = (x_2^j)_e\left[-\left(\frac{1}{2} - \bar{\gamma}_e\right)U_e^* C_E^\rho + \rho_e^* d_e \alpha_e\right]$$

$$A_w = (x_2^j)_w\left[\left(\frac{1}{2} + \bar{\gamma}_w\right)U_w^* C_W^\rho + \rho_w^* d_w \alpha_w\right]$$

$$A_n = (x_2^j)_n\left[-\left(\frac{1}{2} - \bar{\gamma}_n\right)V_n^* C_N^\rho + \rho_n^* d_n \gamma_n\right]$$

$$A_s = (x_2^j)_s\left[\left(\frac{1}{2} + \bar{\gamma}_s\right)V_s^* C_S^\rho + \rho_s^* d_s \gamma_s\right]$$

$$A_P = m_P^\rho C_P^\rho + (x_2^j)_e \rho_e^* d_e \alpha_e + (x_2^j)_w \rho_w^* d_w \alpha_w + (x_2^j)_n \rho_n^* d_n \gamma_n + (x_2^j)_s \rho_s^* d_s \gamma_s$$

$$B_P = \frac{(x_2^j)_P \rho_P^\circ}{J_P\,\Delta t} - m_P^\rho \rho_P^* - (x_2^j)\left(\frac{1}{2} - \bar{\gamma}_e\right)U_e^* \rho_E^* + (x_2^j)_w\left(\frac{1}{2} + \bar{\gamma}_w\right)U_w^* \rho_W^*$$

$$-(x_2^j)_n\left(\frac{1}{2} - \bar{\gamma}_n\right)V_n^* \rho_N^* + (x_2^j)_s\left(\frac{1}{2} + \bar{\gamma}_s\right)V_s^* \rho_s^*$$

$$m_P^\rho = \frac{(x_2^j)_P}{J_P\,\Delta t} + (x_2^j)_e\left(\frac{1}{2} + \bar{\gamma}_e\right)U_e^* - (x_2^j)_w\left(\frac{1}{2} - \bar{\gamma}_w\right)U_w^*$$

$$+(x_2^j)_n\left(\frac{1}{2} + \bar{\gamma}_n\right)V_n^* - (x_2^j)_s\left(\frac{1}{2} - \bar{\gamma}_s\right)V_s^*$$

REFERENCES

1. W. H. Chu, Development of a General Finite Difference Approximation for a General Domain—Part I: Machine Transformation, *J. Comp. Phys.*, vol. 8, pp. 392–408, 1971.
2. A. M. Winslow, Numerical Solution of the Quasilinear Poisson Equation in a Nonuniform Triangle Mesh, *J. Comp. Phys.*, vol. 2, pp. 149–172, 1967.
3. J. F. Thompson, F. C. Thames, and C. W. Mastin, Automatic Numerical Generation of Body-Fitted Curvilinear Coordinate System for Field Containing Any Number of Arbitrary Two Dimensional Bodies, *J. Comp. Phys.*, vol. 15, pp. 299–319, 1974.
4. J. F. Thompson, Z. U. A. Warsi, and C. W. Mastin, *Numerical Grid Generation: Foundations and Applications*, Elsevier, New York, 1985.
5. F. H. Harlow and J. E. Welch, Numerical Calculation of Time Dependent Viscous Incompressible Flow of Fluid with Free Surface, *Phys. Fluids*, vol. 8, pp. 2182–2189, 1965.
6. C. M. Rhie, A Numerical Study of the Flow Past an Isolated Airfoil with Separation, Ph.D. thesis, University of Illinois, Urbana-Champaign, 1981.
7. C. Hsu, A Curvilinear-Coordinate Method for Momentum, Heat and Mass Transfer in Domains of Irregular Geometry, Ph.D. thesis, University of Minnesota, Minnesota, 1981.

8. M. Reggio and R. Camarero, Numerical Solution Procedure for Viscous Incompressible Flows, *Numer. Heat Transfer*, vol. 10, pp. 131–146, 1986.
9. M. Peric, R. Kessler, and G. Scheuerer, Comparison of Finite Volume Numerical Methods with Staggered and Colocated Grids, *Comp. & Fluids*, vol. 16, pp. 389–403, 1988.
10. S. Majundar, Role of Underrelaxation in Momentum Interpolation for Calculation of Flow with Nonstaggered Grids, *Numer. Heat Transfer*, vol. 13, pp. 125–132, 1988.
11. M. C. Melaaen, Calculation of Fluid Flows with Staggered and Nonstaggered Curvilinear Nonorthogonal Grids—The Theory, *Numer. Heat Transfer, Part B*, vol. 21, pp. 1–19, 1992.
12. K. H. Chen and R. H. Pletcher, Primitive Variable, Strongly Implicit Calculation Procedure for Viscous Flows at All Speeds, *AIAA J.*, vol. 29, pp. 1241–1249, 1991.
13. C. H. Marchi, C. R. Maliska, and A. L. Bortoli, The Use of Co-Located Variables in the Solution of Supersonic Flows, *Proc. 10th Brazilian Congress of Mechanical Engineering*, vol. 1, pp. 157–160, 1989.
14. S. V. Patankar, Calculation of Unsteady Compressible Flows Involving Shocks, Mechanical Engineering Dept., Rept. UF/TN/A/4, Imperial College, London, 1971.
15. F. H. Harlow and A. A. Amsden, A Numerical Fluid Dynamics Calculation Method for All Flow Speeds, *J. Comp. Phys.*, vol. 8, pp. 197–213, 1971.
16. J. P. van Doormaal, Numerical Methods for the Solution at Compressible and Incompressible Flows, Ph.D. thesis, University of Waterloo, Waterloo, Ont., Canada, 1985.
17. A. F. C. Silva and C. R. Maliska, A Finite Volume Segregated Formulation for Compressible and or Incompressible Flows in Generalized Coordinates (in Portuguese), *Proc. 2nd Brazilian Thermal Science Meeting*, pp. 11–14, 1988.
18. C. R. Maliska and A. F. C. Silva, A Boundary-Fitted Finite Volume Method for the Solution of Compressible and/or Incompressible Fluid Flows Using Both Velocity and Density Corrections, *Proc. 7th Int. Conf. of Finite Element Methods in Flow Problems*, pp. 405–412, 1989.
19. K. C. Karki and S. V. Patankar, Pressure Based Calculation Procedure for Viscous Flows at All Speeds in Arbitrary Configurations, *AIAA J.*, vol. 27, pp. 1167–1174, 1989.
20. C. H. Marchi, C. R. Maliska, and A. F. C. Silva, A Boundary-Fitted Numerical Method for the Solution of Three Dimensional All Speed Flows Using Co-Located Variables, *Proc. 3rd Brazilian Thermal Science Meeting*, pp. 351–356, 1990.
21. C. R. Maliska and G. D. Raithby, A Method for Computing Three-Dimensional Flows Using Non-Orthogonal Boundary-Fitted Coordinates, *Int. J. Numer. Meth. Fluids*, vol. 4, pp. 519–537, 1984.
22. G. D. Raithby and K. E. Torrance, Upstream-Weighted Differencing Schemes and Their Application to Elliptic Problems Involving Fluid Flow, *Comp. & Fluids*, vol. 2, pp. 191–206, 1974.
23. W. J. Minkowycz, E. M. Sparrow, G. E. Schneider, and R. H. Pletcher (eds.), *Handbook of Numerical Heat Transfer*, Wiley, New York, 1988.
24. S. V. Patankar and D. B. Spalding, A Calculation Procedure for Heat, Mass and Momentum Transfer in Three-Dimensional Parabolic Flows, *Int. J. Heat Mass Transfer*, vol. 15, pp. 1787–1806, 1972.
25. G. D. Raithby and G. E. Schneider, Numerical Solution of Problems in Incompressible Fluid Flow: Treatment of the Velocity-Pressure Coupling, *Numer. Heat Transfer*, vol. 2, pp. 417–440, 1979.
26. J. P. van Doormaal and G. D. Raithby, Enhancements of the SIMPLE Method for Predicting Incompressible Fluid Flow, *Numer. Heat Transfer*, vol. 7, pp. 147–163, 1984.
27. P. Moraes, Jr., and A. A. Neto, Aerodynamic Experimental Investigation of the Brazilian Satellite Launch Vehicle (VLS), *Proc. 3rd Brazilian Thermal Science Meeting*, pp. 211–215, 1990.

28. H. A. Vielmo, A. F. C. Silva, and C. R. Maliska, Conjugate Conduction, Convection and Radiation Problem in Walls Containing Circular Cells, *Proc. 4th Brazilian Thermal Science Meeting*, pp. 363–366, 1992.
29. J. F. V. Vasconcellos, Numerical Simulation of Turbulent Flow in Bifurcating Channels Using Multi-domains (in Portuguese), Master's dissertation, Universidade Federal de Santa Catarina, Florianópolis, SC, Brazil, 1993.
30. C. H. Marchi, A. F. C. Silva, and C. R. Maliska, Numerical Solution of Inviscid Flows in Nozzles with Outlet Supersonic Flow (in Portuguese), *Proc. 4th Brazilian Thermal Science Meeting*, pp. 145–148, 1992.
31. J. L. F. Azevedo, P. Moraes, Jr., C. R. Maliska, C. H. Marchi, and A. F. C. Silva, Code Validation for High Speed Flow Simulation over the VLS Launcher Fairing, *Proc. AIAA 24th Fluid Dynamics Conf.*, 1993, AIAA Paper 93-3046.
32. A. L. Bortoli, C. R. Maliska, and C. S. Barcellos, A Methodology Using Finite Volumes and Finite Elements for Aeroelastic Analysis, *Proc. 4th Brazilian Thermal Science Meeting*, pp. 13–16, 1992.